Proceedings of the 4th WSEAS Int. Conf. on HEAT TRANSFER, THERMAL ENGINEERING and ENVIRONMENT, Elounda, Greece, August 21-23, 2006 (pp331-336)

Heat Transfer Enhancement in Laminar Flow Using Al_2O_3-Water Nanofluid Considering Temperature-Dependent Properties

J. LABONTÉ, C. T. NGUYEN , G. ROY
Faculty of Engineering, Université de Moncton, Moncton, NB, CANADA E1A 3E9

Abstract: - We have numerically studied the problem of laminar flow and heat transfer of Al_2O_3-water nanofluid in a uniformly heated tube, considering temperature-dependent fluid properties. Results have clearly shown that inclusion of nanoparticles into water has produced a considerable heat transfer enhancement; an increase as high as 40% may be achieved with 4% particle concentration. A comparison between a constant and variable property models has been performed, which has shown that, in general, a constant fluid property model tends to underestimate the heat transfer coefficient and to overestimate the wall shear stress.

Key-Words: - Laminar flow, Heat transfer, Heat transfer augmentation, Heat transfer enhancement, Nanofluids, Nanoparticles, Numerical simulation.

1 Introduction

With recent developments in nanotechnologies and manufacturing processes, a new class of fluids, called 'nanofluids', has been created [1]. These rather special fluids, which are usually composed of metallic nanoparticles in suspension in saturated liquids, can constitute an interesting alternative for various heat transfer applications [2], since their thermal conductivities are generally well higher than that of most conventional fluids such as water or engine oils. In fact, some experimental data have shown that an increase of thermal conductivity as much as 150% may be achieved [3-5]. The pioneering experimental works [6-7] have first established the temperature effect on both thermal conductivity and viscosity of nanofluids. Regarding confined flows using nanofluids, pioneering experimental data [8-9] and authors' recent numerical results [10-12] have clearly confirmed the advantageous effects due to a use of such fluids in two specific flow configurations, namely the tube flow and the radial flow between heated disks, as well as for cooling of high heat output microprocessors [13-14]. In these numerical analyses, the assumption of constant properties of nanofluids has been adopted.

In the present work, we have numerically investigated the heat transfer enhancement provided by a particular nanofluid composed of distilled water and Al_2O_3 nanoparticles flowing inside a uniformly heated tube, and this considering dynamic viscosity and thermal conductivity being both temperature-dependent. Some significant results are presented and discussed in this paper.

2 Mathematical Formulation and Numerical Method

We consider the problem of laminar flow and heat transfer inside a straight tube that is submitted to a uniform wall heat flux over its entire length, Fig. 1. The following assumptions have been adopted: the flow is assumed steady and laminar; the nanofluid under study is considered to behave as a homogenous, incompressible, single-phase and Newtonian fluid. For thermal properties of the nanofluid, two different approaches were adopted: an all constant properties (PC model), and a variable properties model (PV model) in which both dynamic viscosity and thermal conductivity of this nanofluid are considered temperature-dependent. Furthermore, both viscous dissipation and compression work are considered negligible.

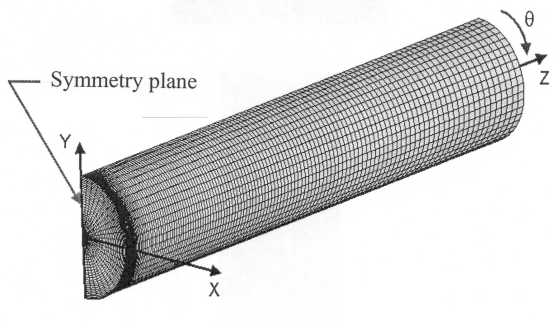

Fig. 1 Geometry of the heated tube considered

Under the above assumptions, the general conservation equations are as follows:

$$div\ (\rho V) = 0 \quad (1)$$

$$div(\rho VV) = -gradP + \mu \nabla^2 V \quad (2)$$

$$div(\rho V C_p T) = div\ (kgradT) \quad (3)$$

where V is fluid velocity vector; P is pressure; k, C_p, ρ and μ are, respectively, fluid thermal conductivity, specific heat, density and dynamic viscosity.

The above equations are subject to the following boundary conditions: i). at the inlet, uniform axial velocity and temperature profiles prevail; ii). at the outlet (at distance 100D from tube inlet), the so-called 'outflow' conditions (zero axial diffusion flux) are imposed, which approximate the fully-developed conditions; iii). at the solid/fluid interface, a usual non-slip conditions prevail, and a constant heat flux q''_W is imposed for the entire tube length; iv). on a vertical plane passing through the tube axis, usual symmetry conditions prevail.

2.1 Thermal Properties of Al_2O_3-Water Nanofluid

By assuming that nanoparticles (ρ_p= 3880 kgm^{-3} and C_p= 773 Jkg^{-1}K^{-1}) are well mixed within the base fluid (water) i.e. their concentration may be considered as uniform throughout the domain, the effective thermal properties of the resulting nanofluid can then be evaluated by using known formulas already developed for classical two-phase mixtures [8, 15]. For the constant properties (PC) model, all nanofluid properties have been evaluated at the fluid inlet temperature using formulas that have been presented and discussed in previous studies, see [8, 10, 13], and are not repeated here for the sake of space. On the other hand, for the variable properties (PV) model, the thermal conductivity k_{nf} (W/mK) and dynamic viscosity μ_{nf} (Pa.s) for two specific particle volume concentrations, 1% and 4%, have been computed using the following formulas [16], which were obtained from the recent experimental data by Das and colleagues [6, 7]:

$$k_{nf} = 0.00335T - 0.3708, \quad \text{for } 1\% \tag{4}$$

$$k_{nf} = 0.00496T - 0.8087, \quad \text{for } 4\% \tag{5}$$

$$\mu_{nf} = 2.9x10^{-7}T^2 - 2x10^{-5}T + 3.4x10^{-2}, \quad \text{for } 1\% \tag{6}$$

$$\mu_{nf} = 3.4x10^{-7}T^2 - 2.3x10^{-4}T + 3.9x10^{-2}, \quad \text{for} 4\% \tag{7}$$

where T is in Kelvin. Regarding the thermal properties of distilled water, they were computed using classical formulas published in [17].

2.2 Numerical Method and Validation

The equations (1-3), which are non-linear and strongly coupled each other, have been successfully solved using a finite-control-volume- based numerical method. The power-law scheme was used throughout to compute the combined 'diffusion-and-convection' fluxes of heat and momentum; the well-known SIMPLE-algorithm has been employed for the treatment of velocity-pressure coupling [18, 19]. In order to ensure the accuracy and the consistency of numerical results with respect to the number of grid points used, several non-uniform grids were extensively tested. The 32x24x155 non-uniform grid – respectively 32, 24 and 155 nodes along R, θ (θ varying from 0° to 180°) and Z directions, with highly packed nodes near all the boundaries - has been found appropriate for the problem studied. The computer code has been satisfactorily validated by comparing numerical results to the corresponding analytical/numerical data for: i). cases of forced convection tube flow and heat transfer and ii). cases of laminar mixed convection flow of water in horizontal tubes. Details regarding the grid sensibility study and the code validation were presented and discussed in [10, 20].

The code was then used to perform numerical simulations for water and water-Al_2O_3 mixtures. As starting conditions, velocity and temperature fields obtained for water cases were used; for subsequent runs, converged solutions for cases of particular particle concentrations were used. For the cases performed in this study, convergence has usually been achieved with residues as low as 10^{-8} (at least) for all the governing equations (1-3).

3 Results and Discussion

Some significant results are shown in the following with emphasis on the effect of variable properties. Unless otherwise noted, the results shown are for the following parameters: q''_W=10240W/m^2; D= 0.05m (tube diameter); L=1m (tube length); the fluid inlet temperature has been fixed to 294K; the Reynolds number (defined as $Re= V_iD\rho/\mu$, V_i is fluid inlet velocity) varies from 250 to 2000, and the particle volume concentrations are respectively, 0% (i.e. without particles), 1% and 4%.

3.1 Axial Development of Thermal Field

Figures 2 and 3 show, respectively, the axial development of wall temperatures and fluid radial temperature profiles obtained for a specific axial location near tube outlet. One can observe, by comparison with the corresponding curve of distilled water, that the inclusion of nanoparticles has clearly produced a beneficial effect on wall temperature T_W, which decreases considerably with an increase of particle concentration, thus obviously indicates a better wall heat transfer rate. It is very interesting to observe that, for a given particle volume concentration, the PV model has consistently produced lower wall temperatures compared to those resulted from the PC model; such a difference appears to be more pronounced towards the tube end. This result can easily be explained by the fact that nanofluid thermal conductivity increases considerably with an augmentation of fluid temperature (see again Equations 4 and 5). We can also say that the results produced by the PV model must be, in principle, much more realistic than those of the PC model. Similar behaviours regarding the effects due to an increase of particle concentration as well as a comparison between PV v/s PC models can be found in Fig. 3 that shows the radial variation of fluid temperature at a particular section near the tube outlet.

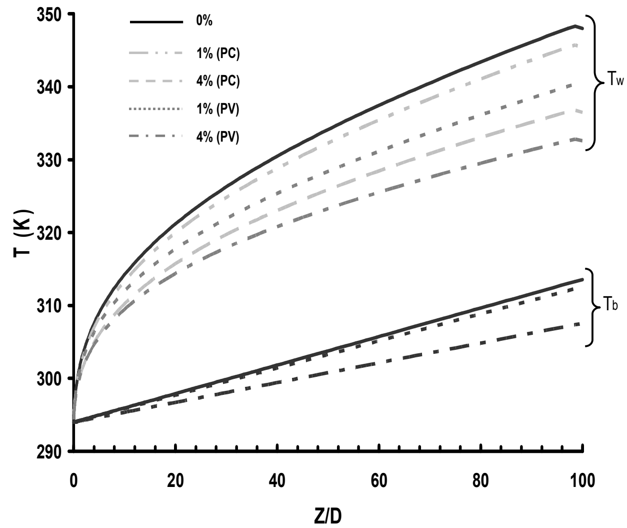

Fig. 2 Axial development of temperatures

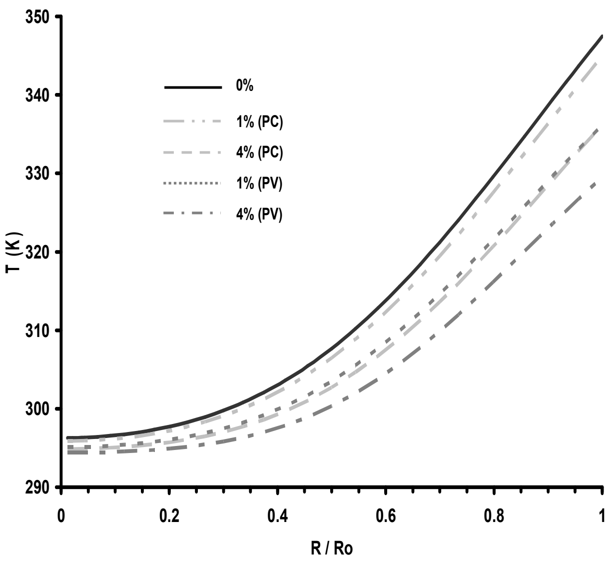

Fig. 3 Fluid temperature profiles near the tube outlet

The heat transfer enhancement along the tube length may be better scrutinised in Figs. 4 and 5, which show, respectively, the axial development of heat transfer coefficient h (W/m^{2}K) and 'nanofluid-to-base fluid' ratio h_r (defined as $h_r = h_{nf} / h_{water}$). It is observed that increasing particle concentration would increase appreciably the heat transfer rate. Thus, for the PV model, respective increases of 20% and 40% have been achieved near the tube outlet, with 1% and 4% concentrations. On the other hand, the corresponding increases, only 5% and 20%, were obtained with the PC model (Fig. 4). In general, one can say that for a given particle concentration, the PV model predicts higher heat transfer rates than the PC model. Such behaviour is obviously due to temperature effect on nanofluid thermal conductivity, as previously stated.

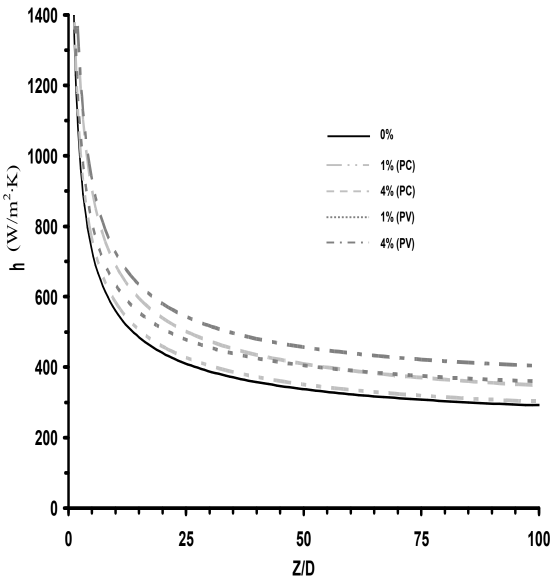

Fig. 4 Variation of local heat transfer coefficient h

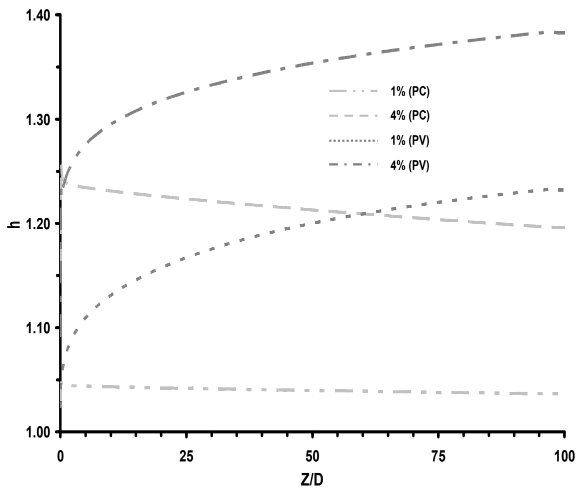

Fig. 5 Variation of heat transfer coefficient ratio h_r

3.2 Averaged Heat Transfer Performance of Nanofluid

Figures 6 and 7 show, respectively, the dependence of $\overline{h}$ and parameter $\overline{h_r}$ ($\overline{h}$ is in fact, the averaged heat transfer coefficient over the entire tube length; $\overline{h_r}$ is the 'nanofluid/base fluid' ratio of averaged heat transfer coefficients) with respect to particle concentration and flow Reynolds number. We can clearly observe that, in general, for water as well as nanofluid studied, $\overline{h}$ increases considerably with an augmentation of *Re*, which appears physically realistic. For nanofluid, $\overline{h}$ also increases appreciably with particle concentration. Thus, for PC model and Re= 500 for example, $\overline{h}$ (W/m^{2}K) has as respective values, 417 and 434 and 508 for water, 1% and 4% concentrations; in counterpart, for PV model, the respective values of $\overline{h}$ are 487 (1%) and 552 (4%). Again, one can observe that PC model has a clear tendency to considerably underestimate the heat transfer rate (Fig. 6). From results in Fig. 7, an enhancement varying from 12% to 20% and, from 28% to 36% may be expected, respectively, for nanofluids with 1% and 4% particle concentrations.

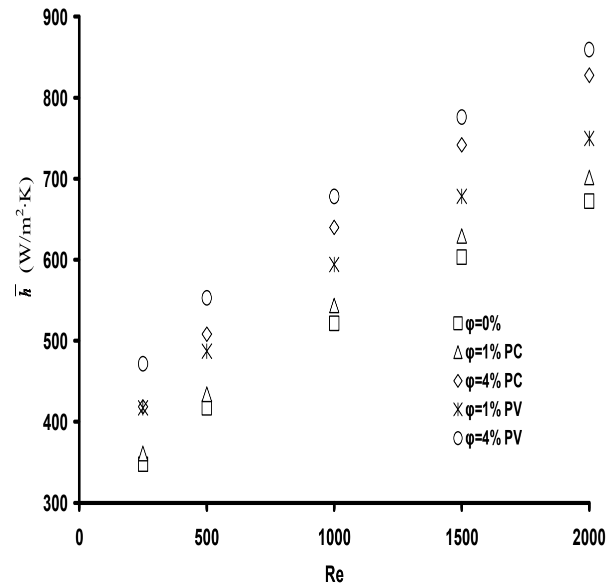

Fig. 6 $\overline{h}$ as function of *Re* and particle volume concentration

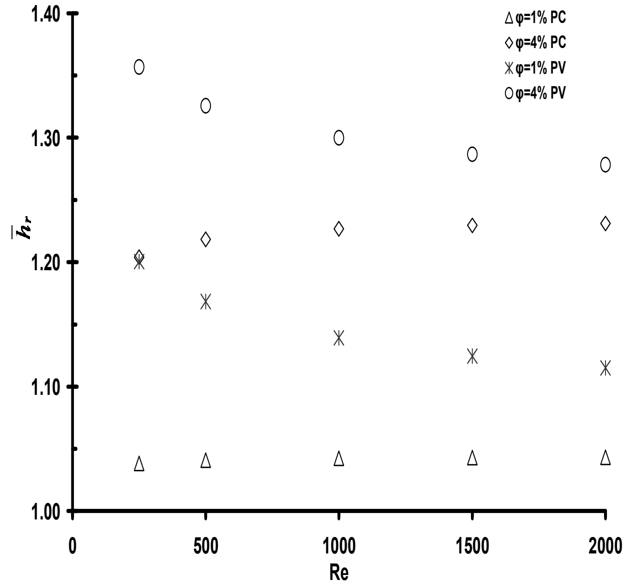

Fig. 7 $\overline{h_r}$ as function of *Re* and particle volume concentration

3.3 Fully-Developed Heat Transfer and Wall Shear Stress

Figures 8 and 9 show the results for $\overline{h}$ (W/m^{2}K) and ratio $\overline{h_r}$ for fully-developed conditions i.e. near the tube outlet. As expected, similar behaviours regarding the heat transfer enhancement with respect to parameter *Re* and particle concentration are again observed here. Also, the underestimation of heat transfer by the PC model is still present. Thus, for PC model, values of $\overline{h_r}$ are almost constant regardless the parameter *Re*: $\overline{h_r}$ =1.04 and ≈1.2 respectively for 1% and 4% concentrations, that is an increase of 4% and ≈20% of heat transfer rate compared to that of water. On the other hand, for PV model, the corresponding increases of heat transfer are, respectively, from 16% to 26% for 1% particle concentration, and from 32% to 42% for nanofluid with 4% particle concentration.

Figure 10 shows, finally, the variation of wall shear stress $\overline{\tau}$ (Pa) as function of parameter *Re* and particle volume concentration. As we can expect, the wall shear stress considerably increases with an increase of flow Reynolds number, which is physically quite realistic. It is also observed that an inclusion of nanoparticles has also increased the wall friction. Such an increase clearly becomes more pronounced with an augmentation of particle

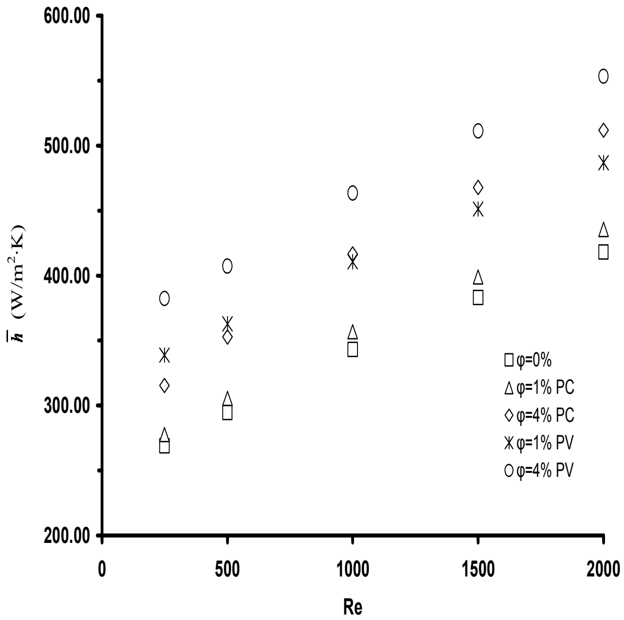

Fig. 8 Values of $\bar{h}$ (fully-developed) as function of *Re* and particle volume concentration

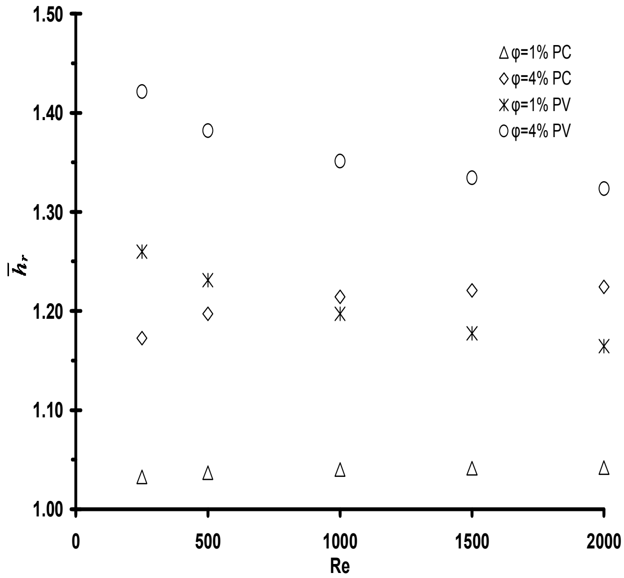

Fig. 9 Values of $\overline{h_r}$ (fully-developed) as function of *Re* and particle volume concentration

concentration, which is directly linked to the increase of nanofluid viscosity with particle loading. From results shown in Fig. 10, it is very interesting to remark that, for given particle concentration, the PC model consistently overestimates wall shear stress while compared to the PV model. Such behaviour is obviously due to the fact that PV model takes into account the temperature effect on nanofluid dynamic viscosity while in PC model, this

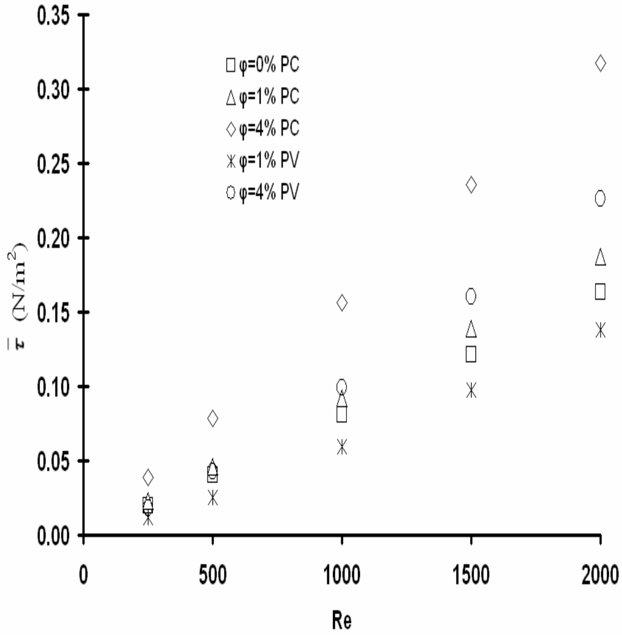

Fig. 10 Values of $\bar{\tau}$ (fully-developed) as function of *Re* and particle volume concentration

property is invariably computed at fluid inlet temperature (fixed at 294K). Far downstream near the tube outlet, fluid temperatures are indeed higher than 294K, and local viscosities are lower than the one computed at 294K (see again Equations 6 and 7). As consequence, the wall shear stresses computed by PV model must be lower than those using PC model. Finally, it appears obvious from results shown that the PC model, not only it considerably underestimates the heat transfer coefficient, but does also overestimate the wall friction. Hence, only the PV model can offer a more realistic evaluation of nanofluid behaviour, and in some ways, has given a just credit to the use of such nanofluids in real thermal applications.

4 Conclusion

In this paper, we have numerically studied, using a constant property and variable property models, the heat transfer enhancement provided by a particular nanofluid, Al_2O_3-water mixture, in a uniformly heated tube. Results have clearly shown that an inclusion of nanparticles into water has produced a considerable heat transfer enhancement, but also an important increase of wall shear stress. Such advantageous effect on heat transfer and disadvantageous one on wall friction have been found to become more pronounced with an augmentation of particle volume concentration and/or flow Reynolds number. It has also been found that a variable property model, for which more realistic results can be expected, has produced, for a given particle concentration, appreciably higher heat transfer coefficients and much lower wall shear stresses than the corresponding ones computed using a constant property model.

Acknowledgement

The authors wish to thank the '*Natural Sciences and Engineering Research Council of Canada*' and the Faculty of Graduated Studies and Research of '*Université de Moncton'* for their financial supports to this project. Thanks are also due to the Faculty of Engineering of '*Université de Moncton'* for allocating computing facilities.

References:

[1] Nanophase Technologies, Romeoville, IL, USA, http://www.nanophase.com

[2] S. Lee, S. U.-S. Choi, Application of metallic nanoparticle suspensions in advanced cooling systems, ASME Publications PVP-Vol. 342/MD-Vol. 72, 1996, pp. 227-234.

[3] J. A. Eastman, S. U.-S. Choi, L. J. Thompson, Anomalously increased effective thermal conductivities of Ethylene Glycol based nanofluids containing copper nanoparticles, *Appl. Phys. Lett.*, Vol. 78, No. 6, 2001, pp. 718-720.

[4] S. U.–S. Choi, Enhancing thermal conductivity of fluids with nanoparticles, developments and application of non-Newtonian flows, ASME FED Vo. 231/MD 66, 1995, pp. 41-46.

[5] X. Wang, X. Xu, S. U. S. Choi, Thermal conductivity of nanoparticles-fluid mixture, *J. of Thermophysics and Heat Transfer*, Vol. 13, No. 4, 1999, pp. 474-480.

[6] N. Putra, W. Roetzel, S.K. Das, Natural convection of nanofluids, *Heat and Mass Transfer*, Vol. 39, 2003, pp. 775-784.

[7] S. K. Das, N. Putra, P. Thiesen, W. Roetzel, Temperature dependence of thermal conductivity enhancement for nanofluids, *J. Heat Transfer*, Vol. 125, 2003, pp. 567-574.

[8] B. C. Pak, Y. I. Cho, Hydrodynamic and heat transfer study of dispersed fluids with submicron metallic oxide particles, *Experimental Heat Transfer*, Vol. 11, No. 2, 1998, pp. 151-170.

[9] Q. Li, Y. Xuan, Convective heat transfer performances of fluids with nano-particles, *Proc. 12th Int. Heat Transfer Conference* (Grenoble, France, August 2002), pp. 483-488.

[10] S. E. B Maïga, S. J. Palm, C. T. Nguyen, G. Roy, N. Galanis. Heat transfer enhancement by using nanofluids in forced convection flows, *Int. J. Heat Fluid Flow*, Vol. 26, 2005, pp. 530-546.

[11] S. E. B. Maïga, C. T. Nguyen, N. Galanis, G. Roy, Heat transfer behaviors of nanofluids in uniformly heated tube, *Superlattices and Microstructures*, Vol. 35, No. 3-6, 2004, pp. 543-557.

[12] G. Roy, C. T. Nguyen, P.-R. Lajoie, Numerical investigation of laminar flow and heat transfer in a radial flow cooling system with the use of nanofluids, *Superlattices and Microstructures*, Vol. 35, No. 3-6, 2004, pp. 497-511.

[13] C. T. Nguyen, G. Roy, P.-R. Lajoie, S. E. B. Maïga, Nanofluids Heat Transfer Performance for Cooling of High Heat Output Microprocessor, Paper No. 530-267, *IASME Transactions*, Issue 6, Vol. 2, ISSN: 1790-031X, 2005, pp. 994-999.

[14] A.-G. Schmitt, T. Maré, C. T. Nguyen, J. Miriel, Étude expérimentale des performances thermiques d'un nanofluide: eau-γAl_2O_3, *Proc. VIIème CIFQ,* St-Malo, France, pp. 223-228, 2005.

[15] Y. Xuan, W. Roetzel, Conceptions for heat transfer correlation of nanofluids*, Int. J. Heat Mass Transfer*, Vol. 43, 2000, pp. 3701-3707.

[16] S. J. Palm, *Étude numérique de l'écoulement et du transfert thermique entre deux disques coaxiaux stationnaires en présence d'un nanofluide,* M. Sc. Thesis, 109p., Université de Moncton, NB, Canada, 2005.

[17] K. D. Hagen, *Heat Transfer with Applications,* Prentice-Hall, 1999.

[18] S. V. Patankar, *Numerical Heat Transfer and Fluid Flow,* Hemisphere/McGraw-Hill, New York, NY, USA, 1980.

[19] Fluent, *Fluent 6 User's Guide,* Lebanon, NH, USA, 2005.

[20] S. E. B. Maïga, *Étude numérique du transfert thermique des 'nanofluides' dans un tuyau chauffé uniformément à la paroi,* M. Sc. Thesis, 96p., Université de Moncton, NB, Canada, 2004.